Local Electron States and Surface Geometry of Si(111)-($\sqrt{3}\times\sqrt{3}$)Ag

E. J. van Loenen, J. E. Demuth, R. M. Tromp, and R. J. Hamers
IBM Thomas J. Watson Research Center, Yorktown Heights, New York 10598
(Received 22 October 1986)

Scanning tunneling microscopy and current-imaging spectroscopy are used to determine the local structural arrangement and stoichiometry of $\sqrt{3}\times\sqrt{3}$ Ag on Si(111). The nature of the local electronic structure and the spatial character of the wave functions observed on an atomic scale lead to a structure consisting of Ag trimers embedded in a Si honeycomb formed by threefold-coordinated Si atoms.

PACS numbers: 68.55.Jk, 68.55.Nq, 73.20.At

Recent advances in scanning tunneling microscopy (STM) have made it possible to image surface electronic states atomically in addition to obtaining topographic information.[1-4] Here we demonstrate that such information provides new insight into the structure and bonding of more complex systems—in this case, the ($\sqrt{3}\times\sqrt{3}$)Ag-Si system. Metal-semiconductor interfaces have attracted wide interest,[5] with the initial stages of interface formation frequently proceeding via such $\sqrt{3}$ structures. Even though this Ag-Si structure has been intensively studied, its geometry, even the surface stoichiometry, remain controversial.[6-17] Our STM spectroscopic measurements of the spatial location and character of the surface-state wave functions for ideal regions of ($\sqrt{3}\times\sqrt{3}$)Ag-Si allow us to pinpoint the key structural and chemical elements of this surface, and lead to a Si-honeycomb model consistent with many previous findings.

The type of scanning tunneling microscope used in these studies is described elsewhere.[18] The UHV chamber (base pressure of 1×10^{-10} Torr) contains the STM, LEED optics, a sample transfer assembly, a W-hairpin Ag-evaporation source, and a sensitive deposition monitor. (300 Hz on the monitor corresponds to $\sim8\times10^{14}$ Ag atoms/cm^2, one monolayer, on the sample as calibrated with use of Rutherford backscattering.) The Si(111) samples were 6-mΩ-cm *n*-doped wafers which were cleaned *in situ* by thermal removal of the native oxide at 1050°C, and characterized by both LEED and STM. The "best" $\sqrt{3}$ structures observed by STM were formed by Ag deposition onto the substrate held at 460°C, at a rate of $\sim$0.5 monolayer/min with the background pressure remaining in the 10^{-10}-Torr range. LEED performed *in situ* during the evaporation at 460°C revealed only a $\sqrt{3}$ structure which was the best after at least one monolayer of Ag deposition. However, even on our "best" surfaces, STM revealed some irregular areas and Ag islands coexisting with larger $\sqrt{3}$ regions. Recent, quantitative ion-scattering measurements for identically prepared $\sqrt{3}$ structures readily distinguish the scattering peak from just the $\sqrt{3}$ regions, and determine its spatially averaged coverage to be 0.89 monolayer.[12] Thus, we believe that the range of surface coverages deduced previously for the Ag-$\sqrt{3}$ structure[6-17] arises from microscopic irregularities associated with differences in sample preparation.

In scanning tunneling microscopy a fine W tip is brought in close proximity (5–10 Å) to the sample and biased to allow electrons to tunnel between them. When the tip, mounted on three orthogonal piezoelectric transducers, is scanned along the surface the tunneling current changes as a result of variations in the overlap between the tip and sample wave functions. The *z* transducer, normal to the surface, is controlled by a feedback circuit so as to keep the tunneling current constant and its voltage is monitored to produce a "topographic" map of the surface. We use the Si(111)(7×7) surface to calibrate the *x* and *y* displacements.

In Fig. 1 we show an STM topograph obtained with a −1.0 V bias applied to the sample (tip grounded) and a tunneling current of 2 nA. Here the depressions are black and the maxima are white, with a black-to-white scale corresponding to 1.5 Å. Hexagonal rings consisting of six maxima separated by $\sim$3.9 Å are clearly resolved to form a honeycomb structure. Indicated is the size of the surface unit cell of the $\sqrt{3}$ structure. This topograph is consistent with some of the atomic features expected from a variety of proposed Ag-honeycomb models, having Ag adatoms[6,8] or embedded Ag atoms.[9-11,14] However, in view of recent studies showing that STM images on Si can be dominated by surface states,[2-4] it is not *a priori* clear what the bumps in Fig. 1 actually correspond to. To understand this we have also performed current-imaging tunneling spectroscopy (CITS)[1,2] and have examined the *I-V* characteristics of this surface. In CITS the sample-tip bias voltage is repetitively ramped during scanning, and the current is measured at each pixel for different bias voltages and a fixed sample-tip distance. These bias-dependent current images provide a two-dimensional map of the surface electronic structure.[19]

In Fig. 2(a) we show a topograph obtained with the feedback stabilized at −2 V and a tunneling current of 1 nA. Some of the simultaneously acquired CITS images are also shown in Figs. 2(b)–2(e). The topograph shows

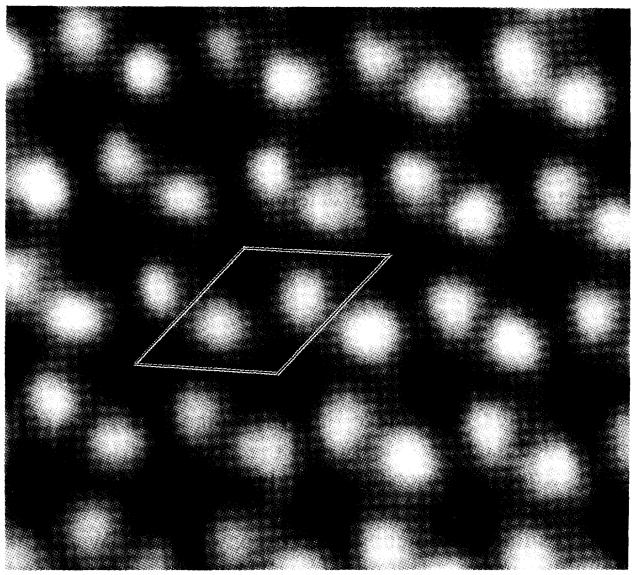

FIG. 1. An STM topograph obtained for a −1-V bias on the sample and a tunneling current of 2 nA. The $\sqrt{3}\times\sqrt{3}$ unit cell is shown and measures 6.65 Å per side. The small distortions of the unit cell arise from thermal drift which we have not corrected for.

much smaller corrugations of ~0.2 Å and implies that the charge density sampled at this bias is relatively smooth across the surface or that the tip is blunt. Our ability to resolve atomic-scale features clearly in the current images excludes the latter, and the current images thereby largely reflect the surface states. Thus, the filled and empty surface states at −1 and +1 V are located on the same sites, and have well-defined onsets or band edges starting at −0.6 and +0.6 V. The empty state remains the same to the highest voltages studied here, +3 V. However, at least two spatially distinct filled states occur: One forms the honeycomb features for biases down to approximately −1.5 V, and the other fills in the honeycomb below −1.5 V.

Another set of STM and CITS scans is shown in Fig. 3 for different tunneling conditions but again with the feedback stabilized at a large negative bias to provide a nearly flat topography. In these CITS images a slightly reduced resolution occurs, and the filled states at −1 V merge together to form "bands" connecting the lattice sites of the honeycomb structure. At −1.6 V [Fig. 3(b)] these bands become more uniform and outline triangular hollows. The empty states remain well resolved which, as discussed later, can be due to the presence of nodal planes in the surface wave functions.

The energies of these two filled and one empty surface state are in overall agreement with previous ultraviolet photoemission spectroscopy[15-17] and bremsstrahlung isochromat spectroscopy[20] measurements. The empty state that we observe starts at ~0.6 eV and persists to higher energies where normal-emission bremsstrahlung isochromat spectroscopy, which samples the Γ point of the surface Brillouin zone, detects this state at 2 eV.[19] This suggests an unoccupied surface state dispersing to lower energies with larger $k_{\parallel}$—as found for 2×1-Si(100),[21] 2×1-Si(111),[22] and $\sqrt{3}\times\sqrt{3}$ Al on Si(111).[23] An important point is that our results, as well as earlier ultraviolet photoemission spectroscopy studies for well-developed $\sqrt{3}$ structures,[15,17] show a surface-state gap at E_F.

Any structural model for $\sqrt{3}$-Ag-Si must account for *both* the STM pattern and the energy and location of the states that we observe. The honeycomb STM features between −1.5 and +3 V can arise from states associated with $\frac{2}{3}$ of a monolayer of Ag or Si atoms. Several Ag-honeycomb models with this coverage have been proposed,[7,9-11,14] but all of these contain an odd number of electrons per $\sqrt{3}$ unit cell and demand a metallic surface—in contradiction to experiments. Alternatively, a top layer of Si atoms can be readily formed in a honeycomb array by creation of one Si vacancy per $\sqrt{3}\times\sqrt{3}$ cell. We propose that three Ag atoms are located about this vacancy in the hollows of the honeycomb where they give rise to the states below −1.5 V. Three silver atoms per $\sqrt{3}$ unit cell allow the surface to be semiconducting and this arrangement is in agreement with recent cover-

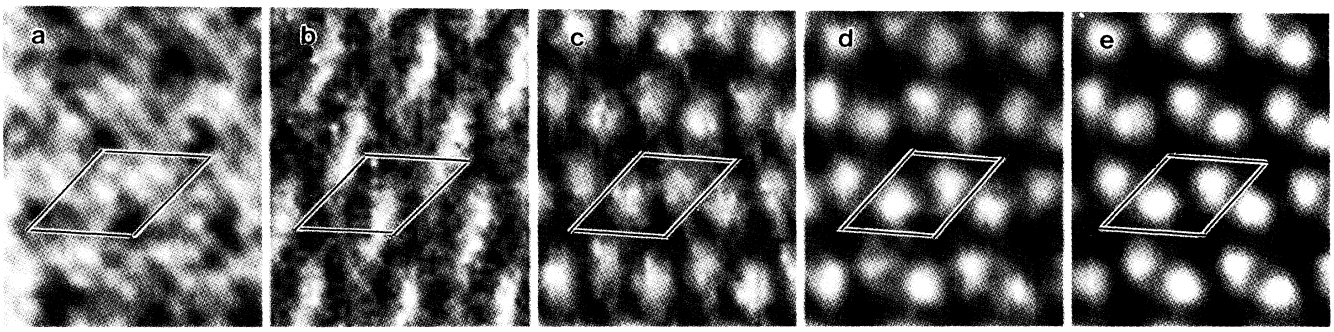

FIG. 2. (a) STM topograph obtained with a −2-V bias and 1-nA tunneling current and (b)–(e) simultaneously acquired current images at −2.5, −1, +1, +2 V bias, respectively. (No corrections have made for thermal drift.)

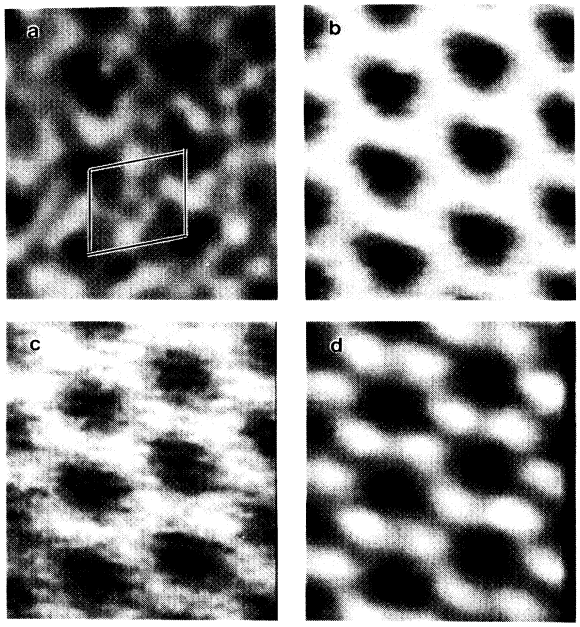

FIG. 3. (a) STM topograph obtained with a −2.5-V bias and 4.8-nA tunneling current and (b)–(d) simultaneously acquired current images at −1.6, −0.9, +1.2 V bias, respectively. (No corrections have been made for thermal drift.)

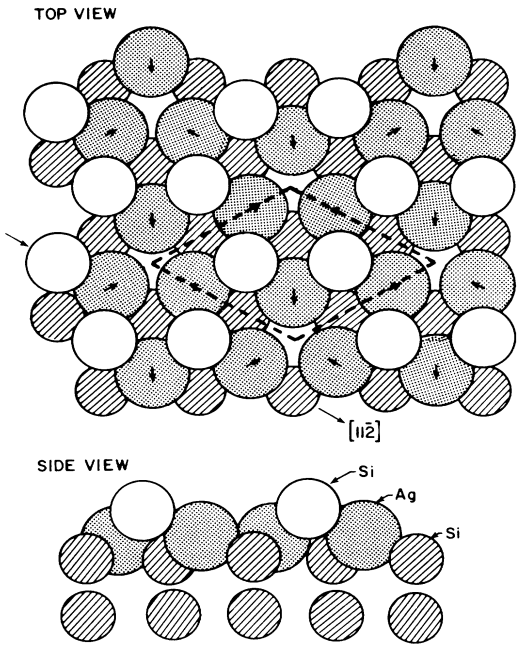

FIG. 4. Top and side views of the embedded Ag-trimer, Si-honeycomb model for the $(\sqrt{3}\times\sqrt{3})$Ag-Si structure. The side view is along a [11$\bar{2}$] direction and the unit cell is indicated by the dashed lines. The arrows on the atoms represent some small displacements that we anticipate from symmetric positions.

age determinations.[12,14] Low-energy ion scattering[9] and extended x-ray-absorption fine-structure polarization-dependent results[11] also indicate that the Ag atoms must reside below the top layer of Si atoms. This leads us to the structural model shown in Fig. 4 which is similar to one of two models favored by the angle-dependent Auger measurements of Horio and Ichimiya.[24] (The other model was Kono's[14] Ag honeycomb structure.) The Ag-Si and Ag-Ag bond distances in our model are consistent with the nearest-neighbor distances determined by extended x-ray-absorption fine structure[11] for the low-coverage $\sqrt{3}$ structure.

The energy separation between the filled and empty states and their location on the same Si atoms has several implications for the bonding and Ag-Si interactions on the surface. Consider the Si surface states to be simple p_z orbitals as on ideally terminated Si(111). In this case this state might be empty, or partially or completely occupied, but it would not exhibit a gap. A gap can arise if these atomic states form bonding and antibonding combinations to produce symmetry differences between the filled and empty states. This is consistent with the gap's opening at the surface-Brillouin-zone boundary, driven by the interactions between Si p states and other states[23]—here presumably the Ag s and p states. Such symmetry changes are expected to introduce nodes in the wave function of the empty states. The fact that the empty and filled states are localized on the same atom also rules out simple charge transfer between Si atoms as occurs between adatoms and rest atoms on Si(111)(7×7)[1,25] or for the dimer atoms on Si(100).[2,21] Our CITS images further suggest that the occupied states have increasing Si-$p_{x,y}$ or Ag character deeper into the higher-lying filled band to produce their more diffuse appearance. The occupied state below −1.5 V which fills in the center of the hexagon would appear to be mainly Ag derived. This state is more complex having an energy-dependent twofold symmetry [Fig. 2(b)], which may be induced by the twofold symmetry of the $\sqrt{3}$ unit cell. We note that we have attempted to observe tunnelings from the known Ag d states but have not seen them, probably because of the shorter decay length of these d wave functions relative to s and p states.

A similar structure having three Au atoms, but bonded atop the surface, has also been proposed for the $\sqrt{3}\times\sqrt{3}$ Au structure on Si(111).[26] The Ag structure that we propose is physically appealing in that the less-electronegative Ag atom is expected to be more of an electron donor than Au and, consequently smaller, which would allow the Ag atoms to fit more readily into the Si lattice.

In summary, we show that the energy structure and spatial character of the surface wave functions spectroscopically probed by STM provide new information by which to understand the structure and bonding of more complex semiconductor surfaces and interfaces.

The authors gratefully acknowledge useful discussions with N. D. Lang, J. Tersoff, and D. DiVincenzo, and thank, in particular, K. C. Pandey for his valuable suggestions. This work is partially supported by the U.S. Office of Naval Research.

[1]R. J. Hamers, R. M. Tromp, and J. E. Demuth, Phys. Rev. Lett. **56**, 1972 (1986).

[2]R. M. Tromp, R. J. Hamers, and J. E. Demuth, Science **234**, 304 (1986).

[3]R. M. Tromp, R. J. Hamers, and J. E. Demuth, Phys. Rev. B **34**, 1388 (1986).

[4]R. M. Feenstra, J. A. Stroscio, and A. P. Fein, Phys. Rev. Lett. **57**, 2579 (1986).

[5]J. H. Weaver, Phys. Today **39**, No. 1, 24 (1986).

[6]F. Wehking, H. Beckerman, and R. Niedermayer, Surf. Sci. **71**, 364 (1978).

[7]G. LeLay, M. Manneville, and R. Kern, Surf. Sci. **72**, 405 (1978); G. LeLay, A. Chauvel, M. Manneville, and R. Kern, Appl. Surf. Sci. **9**, 190 (1981).

[8]J. A. Venables, J. Derrien, and A. P. Janssen, Surf. Sci. **95**, 411 (1980).

[9]M. Saitoh, F. Shoji, K. Oura, and T. Hanawa, Surf. Sci. **112**, 306 (1981).

[10]Y. Terada, T. Yoshizuka, K. Oura, and T. Manawa, Surf. Sci. **114**, 65 (1982).

[11]J. Stohr, R. Jaeger, G. Rossi, T. Kendelewicz, and I. Lindau, Surf. Sci. **134**, 813 (1983).

[12]E. J. van Loenen, M. Iwami, R. M. Tromp, and J. V. Van der Veen, Surf. Sci. **137**, 1 (1984); E. J. van Loenen, to be published.

[13]M. Hanbücken, M. Futamoto, and J. A. Venables, Surf. Sci. **147**, 1433 (1984).

[14]S. Kono, K. Higashiyama, and T. Sagawa, Surf. Sci. **165**, 21 (1986).

[15]D. Bolmont, Ping Chen, and C. A. Sebenne, J. Phys. C **14**, 3313 (1981).

[16]G. V. Hansson, R. Z. Bachrach, R. S. Bauer, and P. Chiaradin, Phys. Rev. Lett. **45**, 1033 (1981), and J. Vac. Sci. Technol. **18**, 550 (1981).

[17]T. Yokotsuka, S. Kono, S. Suzuki, and T. Sagawa, Surf. Sci. **127**, 35 (1983).

[18]J. E. Demuth, R. J. Hamers, R. M. Tromp, and M. E. Welland, J. Vac. Sci. Technol. A **4**, 1320 (1986).

[19]For a theoretical discussion of *I-V* spectra in STM, see N. D. Lang, Phys. Rev. B **34**, 5947 (1986), and Phys. Rev. Lett. **58**, 45 (1987).

[20]J. M. Nicholls, F. Salvan, and B. Reihl, Phys. Rev B **34**, 2945 (1986).

[21]J. Ihm, M. L. Cohen, and D. J. Chadi, Phys. Rev. B **21**, 4592 (1980).

[22]K. C. Pandey, Phys. Rev. Lett. **47**, 1913 (1981), and **49**, 223 (1982).

[23]J. Northrup, Phys. Rev. Lett. **53**, 683 (1984).

[24]Y. Horio and A. Ichimiya, Surf. Sci. **164**, 589 (1985).

[25]J. Northrup, Phys. Rev. Lett. **57**, 154 (1986).

[26]K. Oura, M. Katayama, F. Shoji, and T. Hanawa, Phys. Rev. Lett. **55**, 1486 (1985).

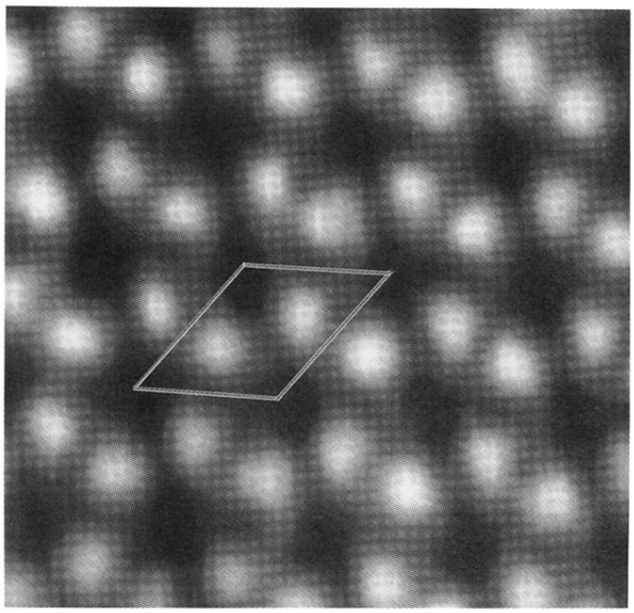

FIG. 1. An STM topograph obtained for a -1-V bias on the sample and a tunneling current of 2 nA. The $\sqrt{3}\times\sqrt{3}$ unit cell is shown and measures 6.65 Å per side. The small distortions of the unit cell arise from thermal drift which we have not corrected for.

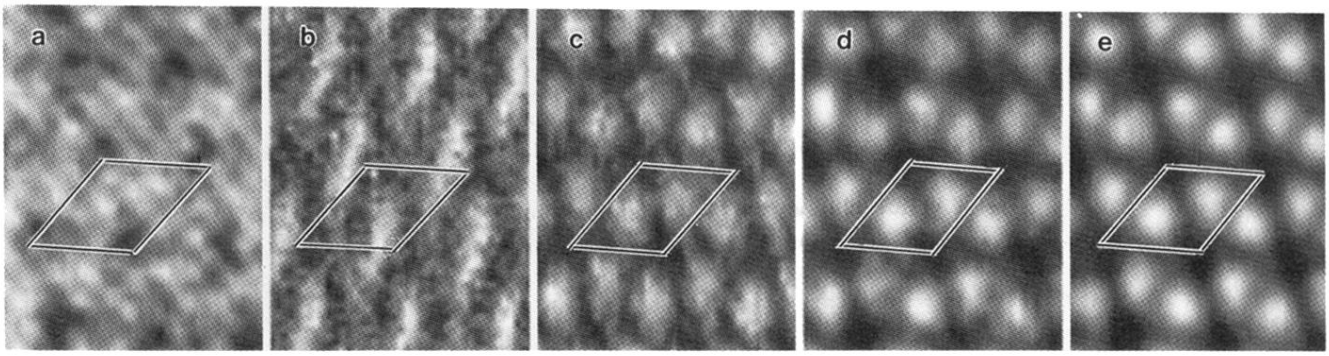

FIG. 2. (a) STM topograph obtained with a −2-V bias and 1-nA tunneling current and (b)–(e) simultaneously acquired current images at −2.5, −1, +1, +2 V bias, respectively. (No corrections have made for thermal drift.)

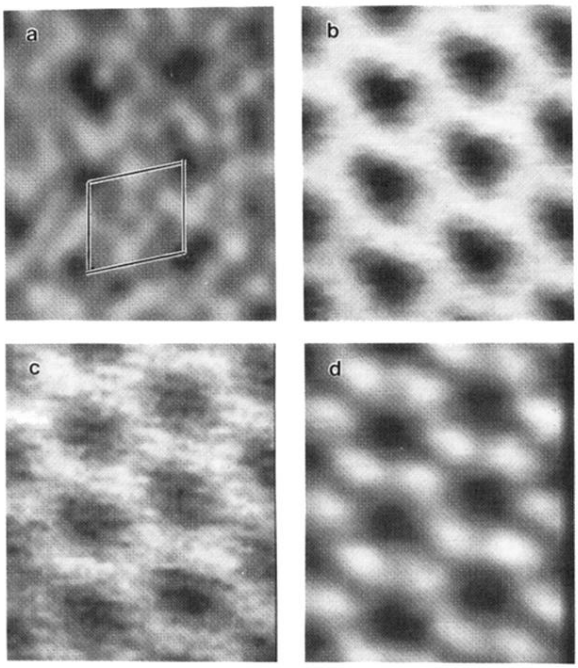

FIG. 3. (a) STM topograph obtained with a −2.5-V bias and 4.8-nA tunneling current and (b)–(d) simultaneously acquired current images at −1.6, −0.9, +1.2 V bias, respectively. (No corrections have been made for thermal drift.)